RSC Advances

Immobilization of laccase on magnetic silica nanoparticles and its application in the oxidation of guaiacol, a phenolic lignin model compound

Journal:	*RSC Advances*
Manuscript ID	RA-ART-07-2015-014982.R1
Article Type:	Paper
Date Submitted by the Author:	31-Oct-2015
Complete List of Authors:	Hu, Jianpeng; Northeast Forestry University, Material Science and Engineering College Yuan, Bingnan; Northeast Forestry University, Material Science and Engineering College Zhang, Yongming; Northeast Forestry University, Material Science and Engineering College Guo, Minghui; Northeast Forestry University, Material Science and Engineering College
Subject area & keyword:	Biocatalysis < Catalysis

RSC Advances

PAPER

Immobilization of laccase on magnetic silica nanoparticles and its application in the oxidation of guaiacol, a phenolic lignin model compound

Received 00th January 20xx,
Accepted 00th January 20xx

DOI: 10.1039/x0xx00000x

www.rsc.org/

Jianpeng Hu, Bingnan Yuan, Yongming Zhang and Minghui guo*

A novel magnetically separable laccase immobilized system was constructed by immobilizing a *Aspergillus* laccase on the core-shell structure of amino-functionalised magnetic silica nanoparticles (AF-MSNPs) via a chemical crosslinking method. A large immobilization capacity (613.5±10.5 mg/g), activity recovery of 53.4±3.1 % and broader pH and temperature profiles than free laccase have been exhibited by the immobilized laccase. Thermal stability, storage stability and operational stability was increased to a great extent. Application of the immobilized system in catalyzing the guaiacol as phenolic lignin model compound was investigated. The high catalytic efficiency for the guaiacol indicated that utilizing the immobilized laccase to catalysis lignin is a very promising technology for further application in the field of wood industry.

1. Introduction

Laccase (benzenediol: oxygen oxidoreductase; EC 1.10.3.2) is an enzyme belonging to the multicopper oxidase family commonly found in plants, insects and bacteria. But the most important source of this enzyme is fungi.[1] Laccase is used for a variety of biocatalytic applications, e.g., the delignification of lignocellulosics, the cross-linking of polysaccharides, bioremediation, waste water bioremediation or textile dye transformation, as well as the manufacturing of forest products.[2]

Traditionally, increasingly expensive petroleum-derived adhesives are required for the fabrication of such forest products, and therefore the manufacturers of medium density fiberboard (MDF), particleboard (PB), and structural panels, for instance, plywood and oriented strand board (OSB), are under pressure to reduce their production costs, the emission of harmful formaldehyde from the adhesives, and to improve product recyclability.[3] Solving these issues requires innovative approaches to minimize the amount of binder while at the same time ensuring a high product quality. In its search for solutions to these challenges, the forest industry is increasingly adopting enzyme-based technologies.[4] The natural origin, non-toxicity, and mild operating conditions of fungi and their enzymes have stimulated several studies on the applicability of fungal enzymes in the forest industry.[5]

Laccase can oxidise lignin, an aromatic polymer that is one of the main components of wood, together with the cellulose and hemicelluloses.[6] Laccase acts on phenolic lignin substrates by catalysing the oxidation of their phenolic hydroxyl groups to phenoxy radicals while dioxygen (O_2) is reduced to water. By the radical polymerisation between these phenoxy radicals, the wood structure units such as wood fibers and wood particles can be bonded together under certain hot-pressing conditions and pressed into the wood-based composites.[7] The enzyme-assisted bonding helps cutting production cost, and reducing formaldehyde emissions from the adhesives during production and end-use of the boards. The laccase treatment of wood fibres and other wood particles before their pressing into composite boards (such as MDF and PB) has been investigated as a means for the fabrication of boards without the use of petroleum-derived wood adhesives.[8-10] Some MDFs prepared on a pilot-plant scale from laccase-treated fibres via the wet- or dry-process showed a superior mechanical strength compared to the control group, meeting the European standards for the internal board strength[11]. However, the laccase treatment is still not widely applied in the wood industry. Firstly, the fabrication of the free enzymes is very expensive and they possess a low stability. Furthermore, the enzyme is difficult to recycle and cannot be reused.

In order to overcome these limitations for a successful industrial application, several research groups were able to successfully immobilize laccase on different support materials (eg. mesoporous carbon, chitosan and polymer fibers).[12-14] The immobilization allows to be easily separated the enzyme from the liquid carrying the reagents and products. In addition, it improves the stability of the enzymes and extends their range of operation, e.g., concerning the pH value, the temperature range, as well as their resistance to detergents.[15] Magnetic bio-separation technology is a promising technology in the support systems for enzyme immobilization, since on the basis of magnetic properties, compared with conventional filtering separation, rapid separation and easy recovery could be reached in external magnetic field, and the capital and

Material Science and Engineering College, Northeast Forestry University, Harbin 150040, China. E-mail:gmh1964@126.com

operation cost could also be reduced.[16] Magnetic silica nanoparticles (MSNPs) has been proved as an appropriate laccase carrier with the desired stability and high reusability via a simple and efficient synthesis process.[17] Silica is one of the most promising carrier materials for the immobilisation of laccase due to its reliable chemical stability, biocompatibility, and reactivity with various coupling agents.[18] Magnetic nanoparticles not only possess the unique features of nano materials, but also magnetic properties that allow for an easy separation and control of the materials with magnetic fields.[19] Recently, Fe_3O_4-based magnetic nanoparticles have received much attention due to their unique superparamagnetic properties and simple preparation process. The typical method to prepare MSNPs is based on the Stöber process.[20] However, several studies have shown that the MSNPs synthesis process is relatively long,[18,21] and therefore not suitable for a large-scale industrial application. Furthermore, to the best of our knowledge, studies on the use of immobilized laccase to catalysis lignin, and through the radical polymerization to fabricate the wood composite materials have not been reported.

In view of these problems, in this paper, we propose a facile and efficient method for the synthesis of MSNPs for the subsequent immobilisation of *Aspergillus* laccase. The report includes a systematic characterization of the morphology, chemical composition and crystal structure of the synthesis products. Effects of pH and temperature on the laccase activity were investigated. The pH-activity and temperature-activity profiles were evaluated and the thermal stability, storage stability and operational stability of the laccase were also tested. Finally, the catalytic efficiency for oxidation of the guaiacol as lignin model compound by the immobilized laccase was also investigated.

2. Experimental

2.1. Materials

A fungal laccase from *Aspergillus* was purchased from Huamaike Bio-Technology Co. Ltd. (Beijing, China). 2, 2'-azinobis (3-ethylbenzthiazoline-6-sulfonic acid) (ABTS), 3-Aminopropyltriethoxysilane (APTES) and Guaiacol ($C_7H_8O_2$) were purchased from Sigma–Aldrich (USA). All other chemicals were of analytical grade. High-purity water was used for preparation of all aqueous solutions.

2.2. Synthesis and surface engineering of carbon-based magnetic carriers

The Fe_3O_4 nanoparticles were synthesized according to the chemical coprecipitation method.[18,21] Under vigorous mechanical stirring, 100 mL of a freshly prepared aqueous mixture of ferric chloride ($FeCl_3$•6 H_2O, 0.02 M) and ferrous chloride ($FeCl_2$•4 H_2O, 0.01 M) was quickly added into a sodium hydroxide solution (100 mL, 0.10 M), immediately resulting in the precipitation of a black solid. After 60 min, the precipitate was isolated from the solution by magnetic decantation and washed with de-ionized water (3×300 mL) and ethanol (3×300 mL) until a neutral pH value was obtained. Next, the silica was coated on the magnetic Fe_3O_4 core according to a modified Stöber process.[22] 5 mL of TEOS was first dissolved in the reaction system. After the solution in the flask was heated to 30 °C under mechanical stirring, the system was left to react for 10 min. Then, 42 ml of Fe_3O_4 nanoparticles (12 mg/mL in an ethanol solution) was added to the flask. The system was left to react under stirring for 6 h, resulting in a colloidal suspension of magnetic silica nanoparticles (MSNPs). The solid phase was separated by centrifugation (8000 rpm, 6 min). After removal of the liquid, the MSNPs were washed with de-ionized water (3×100 mL) and ethanol (3×100 mL) until a neutral pH value was obtained. To modify the surface of MSNPs with amino groups, 100 mg of the MSNPs were first suspended in a 250 mL three-neck flask with 50 mL of ethanol and 5 mL de-ionized water under low frequency ultrasound at room temperature for 10 min. The flask was sealed with a septum, and the solution was heated to 30 °C under mechanical stirring. 0.2 mL of APTES was injected into the flask and the mixture was allowed to react under stirring for 12 h. Then, the amino-functionalised MSNPs (AF-MSNPs) were separated by magnetic decantation. After removal of the liquid, the AF-MSNPs were washed with de-ionized water (3×100 mL) and ethanol (3×100 mL) until a neutral pH value was obtained. The prepared AF-MSNPs were dried in a vacuum oven at 70 °C for 24 h and stored at 4°C in the refrigerator.

2.3. Laccase immobilization

20 mg of the AF-MSNPs were suspended in a 50 mL flask containing 10 mL glutaraldehyde (5 % v/v) at room temperature and stirred for 6-8 h to increase the amount of aldehyde groups on the surface of the AF-MSNPs. Then the solid was separated by magnetic decantation and rinsed with phosphate-buffered saline (PBS, 0.1 mol/L, pH 7, 2×100 mL), and de-ionized water (2×100 mL) to remove the remaining glutaraldehyde. Next, 15 mL of laccase solution (1 mg/mL in PBS) was added to the flask. The system was left to react under stirring in an ice-water bath at a temperature of 3-5 °C for 20 h. The laccase immobilized on AF-MSNPs was subsequently separated by magnetic decantation to remove the liquid, washed with PBS (100 mL, 0.1 mol/L, pH 7), sodium chloride solution (100 mL, 0.5 mol/L) and de-ionized water (100 mL). The washing process was repeated three times to make sure that there were no free proteins remaining. The obtained immobilized laccase was suspended in PBS (0.1 mol/L, pH 7) and stored at 4 °C. The solidified form of the immobilized laccase was obtained using a vacuum freeze dryer.

2.4. Assay of laccase activity

The activity of free and immobilized laccase was determined spectrophotometrically in a reaction medium containing 2 mL of ABTS (1 mmol/L) as substrate in 2 mL sodium citrate buffer (0.1 mol/L, pH 4.0) at 25 °C in the absorbance at 420 nm.[23] The oxidation of substrate to $ABTS^+$ was measured for 5 min using a double-beam UV-visible spectrophotometer (TU-1900,

Beijing Puxi, China). One unit (U) of laccase activity was defined as the amount of laccase required to oxidize 1 μmol of ABTS per minute.[24] The final activity of immobilized laccase was expressed in U/mg. The activity recovery of the immobilized laccase is calculated from the following formula:

$$R\ (\%) = (A_i / A_f) \times 100$$

Where R is the activity recovery of the immobilized laccase (%), A_i is the activity of laccase immobilized on AF-MSNPs (U), and A_f is the activity of the same amount of free laccase in solution as that immobilized on particles (U).

The effect of pH on the activity of the free and immobilized laccase was determined as the relative activity under the variety of pH range 3.0–8.0 at 25 °C. The optimum temperature of free and immobilized laccase was measured in a temperature range 25–70 °C at a pH of 3.5. Relative activity was calculated as the ratio of the laccase activity measured at a specific pH and temperature to the maximal activity of the laccase in each group of assay.

2.5. Stability of free and immobilized laccase

The thermal and pH stability studies on the free and immobilized laccase were determined by measuring the residual activity of laccase at 25 °C after being incubated at different temperature (30-70 °C) in PBS buffer (pH 7.0) for 2h, and different pH of buffer (pH 3-11) for 12h, respectively, and then taken for the activity measurement.

Storage stability experiments were conducted to determine the stabilities of free and immobilized laccase after storage in PBS buffer (pH 7.0) for 30 days, and then taken for the activity measurement at three days interval. Relative activity was calculated as the ratio of the laccase activity measured in each interval to the initial laccase activity.

The operational stability of the immobilized laccase was assessed by performing ten consecutive operating cycles using ABTS as substrate at 25 °C. At the end of each cycle, the immobilized laccase was separated with a magnet, washed three times with sodium citrate buffer (pH 3.5), and repeated with a fresh aliquot of substrate. Relative activity was calculated as the ratio of the laccase activity measured in the *n*th cycle to the first cycle of laccase activity.

2.6. Catalysing the oxidation of guaiacol by immobilized laccase

Lignin is a three dimensional structure of high polymer combining together with the phenlpropane structure units through the carbon-carbon double bond and ether bond. Due to the complex structure of lignin, the lignin model compounds had been used in many lignin studies.[25] Because of the phenolic lignin was the specific substrate for laccase, the typical phenolic lignin model compound of guaiacol was selected to calculate the catalytic efficiency by the immobilized laccase in this study.

Experiments in catalysing the oxidation of guaiacol was performed at 40 °C with laccase-immobilized in sodium citrate buffer (pH 3.5) under mechanical stirring. 10.0 mg of the immobilized laccase was added into 20 ml reaction medium with 2 mM guaiacol, with incubation time lasting for 1 h. The percentage of guaiacol catalytic oxidation efficiency was determined at different intervals by separating the immobilized laccase with magnet, and then the absorbance of the upper solution was determined using a UV–visible spectrophotometer at 470 nm.[26] The catalytic oxidation efficiency was calculated as the ratio of the absorbance of the upper solution measured at different intervals to the maximal absorbance of the upper solution.

2.7. Characterization

Scanning electron microscopy (SEM) was conducted on a FEI Sirion 200 microscope (USA) operating at 10-20 kV. The SEM samples were prepared by dispersion in ethanol at room temperature; a drop of the supernatant dispersion was then placed onto a tinfoil supported by a piece of copper. The surface element composition was determined using an energy dispersive X-ray spectrometer (EDX, USA). Transmission electron microscopy (TEM) was performed on a JEOL-JEM 2100 microscope operated at 200 kV. The TEM samples were prepared by dispersion in ethanol at room temperature; a drop of the supernatant dispersion was then placed onto a 200-mesh carbon-coated copper grid. Fourier transform infrared (FTIR) spectra were recorded on a Nicolet Magna-IR560 E.S.P. FTIR spectrometer in the range from 400 to 4000cm^{-1} using KBr pellets. For the pellet preparation, KBr was crushed and mixed with a small amount of the solid samples, and the spectra were then recorded at a resolution of 4 cm^{-1} by accumulating 32 scans. X-ray diffraction (XRD, D/max 2200, Rigaku, Japan) with Cu Kα radiation (λ = 0.15406 nm) was performed at 40 kV and 30 mA in the 2θ range from 5 to 80°, with the scan rate set to 5° min^{-1}.

3. Results and discussion

3.1. Characterization of magnetic carbon-based carriers

FTIR experiments were carried out to clarify the chemical structure of both nanoparticles and the carbon-based carries. AS shown in Fig. 1a. The peak at 570.6 cm^{-1} corresponds to the Fe-O stretching vibration characteristic for Fe_3O_4.[27] The peak at 3424.6 cm^{-1} corresponding to the O-H stretching vibration is attributed to the hydroxyl groups covering the surface of the particles.[28] The three bands at 469.2, 797.0, and 1101.5 cm^{-1} dominate the spectra obtained for the silica sample and are attributed to the stretching and bending vibrations of silicon and oxygen (Fig. 1b). The peak at 1101.5 cm^{-1} corresponds to the asymmetric Si-O-Si vibrations, whereas the peak at 797.0 cm^{-1} is ascribed to the symmetric Si-O-Si stretching vibration and the peak at 469.2 cm^{-1} corresponds to the Si-O bending vibration.[29] The peak at 1633.8 cm^{-1} corresponds to the H-HO bending vibration and the peak at 952.3 cm^{-1} corresponds to the Si-OH bending vibration. Fig. 1c shows the FTIR spectrum obtained for the MSNPs prepared using 2:1 of SiO_2 to Fe_3O_4 mass ratio. The three bands at 469.2, 797.0, and 1101.5 cm^{-1} dominate the spectrum of the silica are obvious. However, the

intensity of the characteristic Fe_3O_4 absorption peak at 570.6 cm^{-1} retained at a low level. After being modified with APTES (Fig. 1d), the intensity of the absorption peak around at 3400 cm^{-1} was obviously increased, which can be attributed to the N-H stretching vibration.[30] The intensity of the absorption peak around at 1650-1500 cm^{-1} was also increased corresponding to the N-H bending vibration. The new bands were observed at 2940 and 2860 cm^{-1} corresponded to -CH_2- stretching vibration and -CH_3 stretching vibration, respectively.

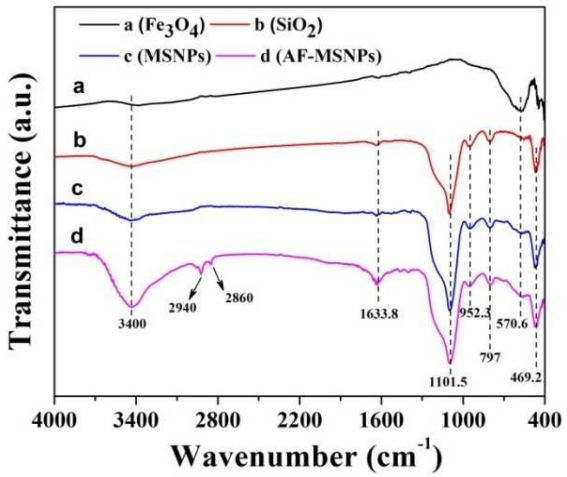

Fig. 1 FTIR spectra of (a) Fe_3O_4; (b) SiO_2; (c) MSNPs; (d) AF-MSNPs.

The X-ray diffraction experiments were carried out to clarify the crystal structure of both nanoparticles and the carbon-based carries. As shown in Fig. 2a, the XRD pattern obtained for the spherical SiO_2 nanoparticles synthesized via a modified Stöber process. This pattern reveals the amorphous nature of the SiO_2 samples. The strong silica peak at 2θ = 24° reflects the amorphous nature of the particle due to the smaller particle size effect and incomplete inner structure of the spherical nanoparticels.[28] No other SiO_2 or impurity peaks were found, indicating a high purity of the spherical SiO_2 nanoparticles. Six diffraction peaks were observed in the range from 20 to 70° (Fig. 2b). The intense peaks at 2θ = 30.24, 35.58, 43.18, 53.82, 57.16 and 62.72° correspond to the (220), (311), (400), (422), (511) and (440) crystal face, respectively, which is agreement with the standard Fe_3O_4 XRD data (JCPDS, card 89-0950).[31] No other Fe_3O_4 or impurity peaks were found, indicating that the Fe_3O_4 nanoparticles feature a single-phase spinel structure. The FTIR spectra together with XRD pattern confirmed that the particles synthesized in this study were pure Fe_3O_4 nanoparticles. The MSNPs and AF-MSNPs obtained the similar XRD pattern (Fig. 2c and d). Diffraction peaks attributed to both SiO_2 and Fe_3O_4 were founded in the patterns, which indicated that the amino modification has no effect on the crystal structure of the MSNPs. However, the XRD patterns of the MSNPs and AF-MSNPs displays Fe_3O_4 peaks of lower as compared with Fe_3O_4, especially for the peaks at 2θ = 30.24, 43.18 and 53.82°. This is probably due to the presence of silica layers were grown on the surface of the Fe_3O_4.[21]

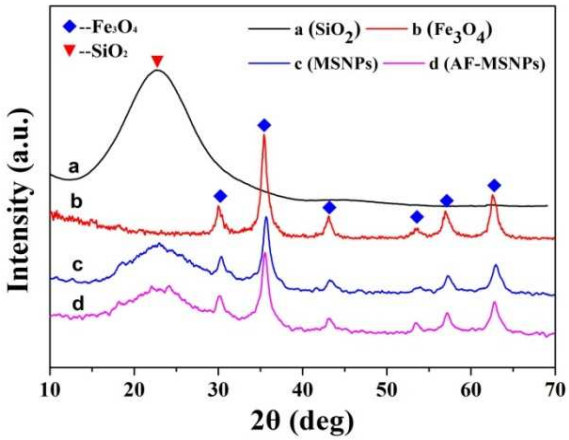

Fig. 2 X-ray powder diffraction of (a) SiO_2; (b) Fe_3O_4; (c) MSNPs; (d) AF-MSNPs

Fig. 3 illustrates the SEM images of the MSNPs prepared using 2:1 of SiO_2 to Fe_3O_4 mass ratios and the AF-MSNPs. Spherical morphology is evident after Fe_3O_4 coating with silica with a slight of agglomerations (Fig. 3a), as expected for silica-coated magnetic particles prepared by the sol-gel hydrolytic process in basic medium.[30] After the amino modification, the spherical morphology of the AF-MSNPs was unchanged (Fig. 3b). The surface chemical compositions of the samples were determined via SEM-EDX (Table 1). The results showed that the oxygen, silicon and iron existing in MSNPs. Besides above three elements, the carbon and nitrogen were also detected in AF-MSNPs, which indicated that the APTES was successfully grafted to the surface of the MSNPs.

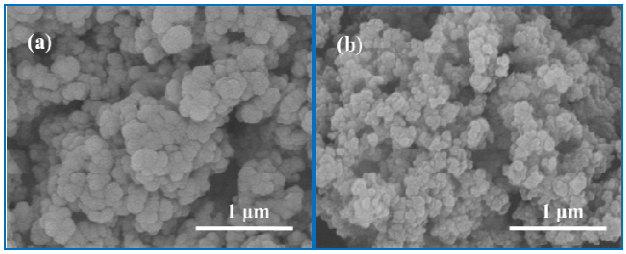

Fig. 3 SEM images of (a) MSNPs and (b) AF-MSNPs.

Table 1. Element content according to the SEM-EDX analysis

Samples	Element content (*Wt* %)				
	O	Si	Fe	C	N
MSNPs	35.04	38.00	26.96	-	-
AF-MSNPS	35.87	20.92	11.37	25.64	6.20

Fig.4 shows the TEM images of MSNPs and AF-MSNPs. The silica completely covers the Fe_3O_4 nanoparticles and formed a core-shell structure of MSNPs (Fig.4a). After the amino modification, the AF-MSNPs could be also observed core-shell structure (Fig.4b). We were able to easily separate the particles from the reaction medium by attracting it with a magnet within 15 seconds.

Based on above results, it confirmed that the silica has been coated on Fe_3O_4 surface, and the MSNPs have been

successfully modified by amino groups. This is a solid foundation for the laccase immobilization and its application discussed later in this work.

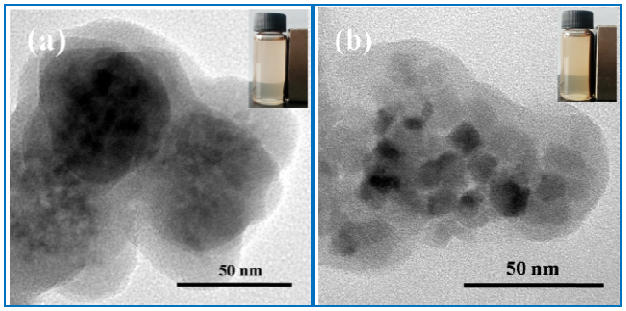

Fig. 4 TEM images of (a) MSNPs and (b) AF-MSNPs. The inserts are the magnetic performance of the magnetic carriers.

3.2 Synthesis mechanisms of the immobilized laccase

The proposed mechanisms for the synthesis of the immobilized laccase are summarized in Scheme 1.

Synthesis of primary particles. During the modified Stöber process, the hydrolysis of TEOS results in the formation of a supersaturated silicic acid solution, which then condensates to small primary silica particles with a diameter below 5 nm. The primary particles are colloidally unstable and are aggregating into larger particles with the surface charge large enough to prevent an irreversible Brownian aggregation.[32]

The overall primary silica particles synthesis reaction via hydrolysis and condensation of TEOS in a solution containing water, methanol, and ammonia is given by Eq. (1).

$$Si(OR)_4 + 2H_2O \rightarrow SiO_2 + 4ROH \qquad (1)$$

The monomer addition growth model and the aggregation growth model are usually used to explain the formation and growth mechanism of such particles. However, a combined model was proposed suggesting that the final particle growth occurs via both monomer addition and the aggregation of primary particles, which is supported by the experimental results as well as theoretical simulations. The TEOS sol–gel process under strongly basic conditions yields amorphous materials which typically display a spherical shape due to the random addition of monomers to the surface of the secondary particles. Using a weak base like ammonia as the catalyst ensures the desired geometry. Furthermore, in order to prepare spherical and monodisperse particles, the initial TEOS and ammonia concentrations must not be too high.[33]

Synthesis of MSNPs. The Fe_3O_4 nanoparticles were added to the reaction solution at an appropriate time during the aggregation of the primary silica particles. When the amount of primary silica particles was sufficient, the Fe_3O_4 nanoparticles may be surrounded by the primary silica particles, and further deposition of silica may allow the formation of the MSNPs. The overall Fe_3O_4 nanoparticles synthesis reaction via the chemical coprecipitation method is given by Eq. (2).

$$Fe^{2+} + 2\,Fe^{3+} + 8\,OH^- = Fe_3O_4 + 4H_2O \qquad (2)$$

Amino-functionalized MSNPs. APTES was used to amino-functionalise the MSNPs via a condensation reaction between the hydroxyl groups on the surface of the MSNPs and the ethoxyl groups of the APTES.

Laccase immobilization. Glutaraldehyde is generally the cross-linking agent used for immobilizing laccase. Due to its small size, it could easily penetrate the internal structure of the protein and react with the amino residues.[34] The Schiff base condensations between the aldehyde groups of the glutaraldehyde and the amino group of the AF-MSNPs and the protein, respectively, have achieved the immobilisation of laccase on the surface of the AF-MSNPs.

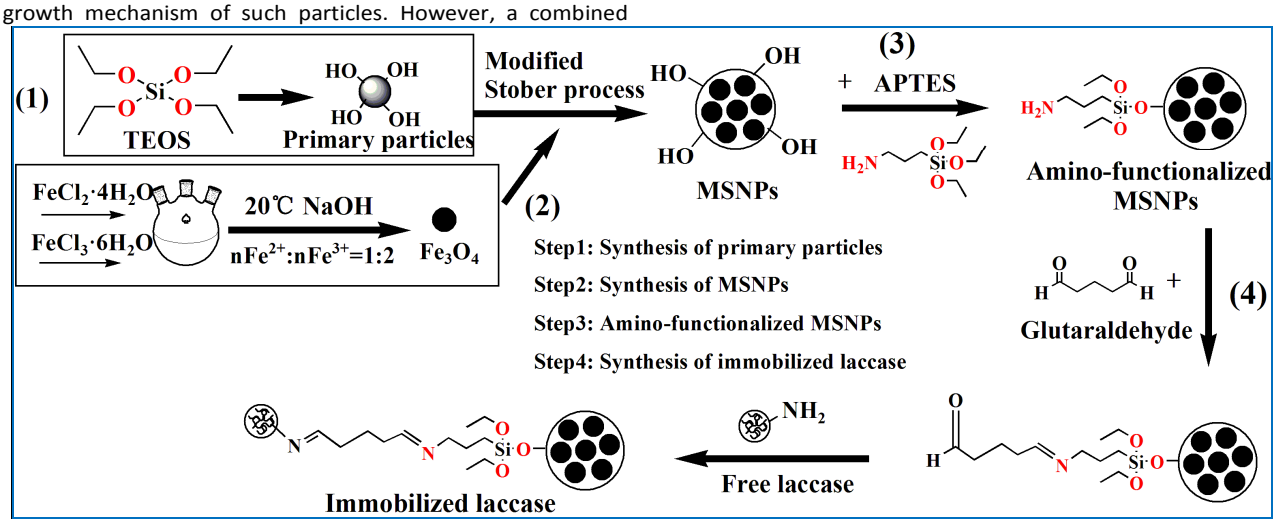

Scheme 1. The synthesis mechanism of the immobilized laccase.

3.3. Laccase activity and properties

3.3.1 Activity of free and immobilized laccase

The enzyme activity was studied using ABTS as substrate. The AF-MSNPs samples synthesized by 2:1 mass ratio of SiO_2 to Fe_3O_4 and modified by 0.2 mL APTES was used for laccase immobilization. The average activity of free laccase was $(1.465\pm0.025) \times 10^{-3}$ U, and the average activity of immobilized

laccase was (4.66±0.16) × 10^{-5} U/mg of settled carrier particles. The activity recovery obtained from immobilized laccase was around 53.4±3.1 % when the initial laccase concentration was 1.0 mg/ml and the immobilized amount of laccase was 613.5±10.5 mg/g of settled carrier particles. Compared to the physical adsorption,[35] the chemical crosslinking method could immobilize more laccase on the surface of carrier particles due to the strong covalent bond between the laccase and carriers.[36] However, a certain decreasing of recovery activity was probably due to a reduction in molecular mobility and comformational changes by the chemical crosslinking.[37]

3.3.2 Effect of pH and temperature on laccase activity

Effect of pH on the activity of free and immobilized laccase on AF-MSNPs was measured at different pH values varying from 3.0 to 5.5 at 25 °C (Fig. 5). The buffer used was sodium hydrogen phosphate-citric acid. The optimum pH of the free laccase was at pH 4.5, which shifted to pH 3.5 for immobilized laccaase. It was attributed to the ionic interaction between laccase and charged surface of the support and the structural conformational change which reflected the relative activity of the enzyme.[36] This phenomenon was also observed in an immobilized laccase on the magnetic bimodal mesoporous carbon[12] and magnetic mesoporous silica nanoparticles.[19] In comparison with the free laccase, the immobilized lacase exhibited more than 60% of the maximum activity with a wider pH range between 3.0 and 5.0. The good pH resistance of the immobilized laccase was due to the stabilization of laccase molecules through covalent attachment was facilitated by strong-binding interactions between the laccase and the amino groups on the surface of the MSNPs. In addition, the structure of the immobilized laccase reduced the occurrence of drastic conformational changes compared to free laccase.[15]

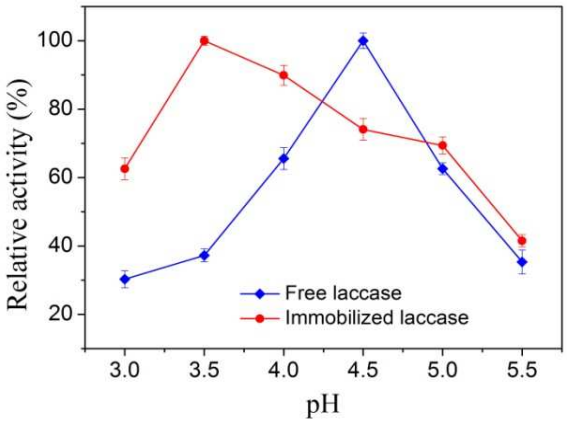

Fig. 5 Effect of pH on the activity of free and immobilized laccase

Relative activities of both the free and immobilized laccase as a function of temperature were compared in Fig. 6. The optimal catalytic temperature was 40 °C for the free laccase and 50 °C for the immobilized laccase. This shift toward high temperature for the immobilized laccase was related to ionic interaction which caused an increase in the activation energy of the laccase to reorganize an optimum conformation for binding to its support.[38] However, in comparison with the free laccase, the immobilized enzyme exhibited a significantly broader temperature profile and its relative activity maintained over 70% for the immobilized enzyme could be observed within the temperature range of 30-60 °C. The improvement in resistance against temperature was probably due to a reduction in molecular mobility and comformational changes by immobilized on AF-MSNPs support.[37]

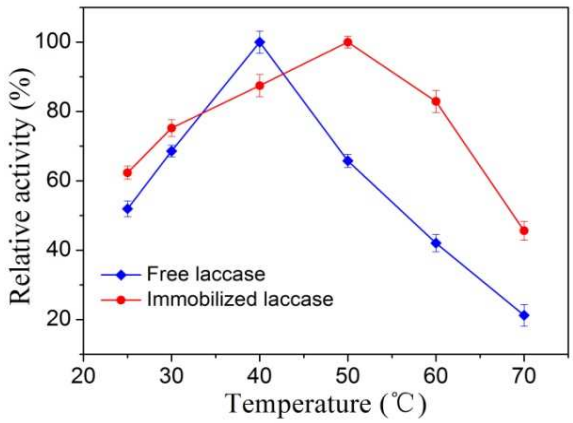

Fig. 6 Effect of temperature on the activity of free and immobilized laccase

3.3.3 Stability of laccase

To determine the effect of the thermal stability on free and immobilized laccase, all samples were incubated at different temperatures (30–70 °C) in PBS buffer solution (0.1 M, pH 7.0) for 2 h. As demonstrated in Fig. 7, the free laccase and immobilized laccase have the similar thermal stability curves. With the increase of incubation temperature, the activity of enzyme decreased sharply. Approximately 40% of the relative activity for free laccase was remained after being incubated at 50 °C for 2 h, but the immobilized laccase still kept about 98% of the relative activity. The free laccase nearly lost its relative activity after incubation at 70 °C for 2 h. In contrast, the immobilized laccase kept about 12% of its whole relative activity under the same condition. The covalent attachment between the laccase and AF-MSNPS seems to protect the enzymatic configuration from distortion or damage by heat exchange and as a result, insolubilized enzymes could work in tougher environment with minimal activity loss.[39] This result indicated that the immobilized laccase was more stable than the free laccase when incubated at high temperature. Hence, the excellent thermal stability makes the immobilized enzyme more economical for its applications in industry.

Storage stability is a significant parameter for carriers applied in biotechnology processes. Storage stability is an imperative advantage of immobilized enzyme over free enzyme because free enzymes can lose their activities fairly quickly. The free and immobilized laccase were stored in PBS buffer solution (1.0 M, pH 7.0) at 4 °C for 30 days and the oxidation activity was determined every three days. As shown in Fig. 8, the free laccase kept about 60% of its initial activity after 9 days, whereas the immobilized laccase still maintained over 90% of its initial activity. The free laccase lost 100% of its initial activity after 18 days, whereas the immobilized laccase retained 79.25 % of its initial activity. After the 30 days of storage, the lacase immobilized on AF-MSNPs remained its 60.35% of its original activity. This result indicates that the storage stability of the immobilized laccase is considerably higher compared with the free laccase. The improved thermal and storage stability of the immobilized laccase was due to increasing stabilization of its active conformation by multipoint

bond formation between the AF-MSNPs support and the laccase molecules.[40]

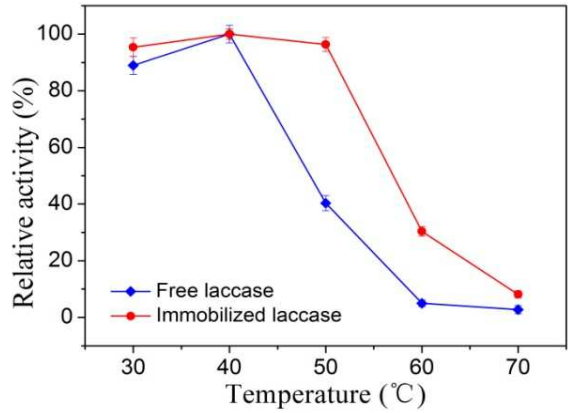

Fig. 7 The thermal stability of free and immobilized laccase incubated at different temperature for 2h

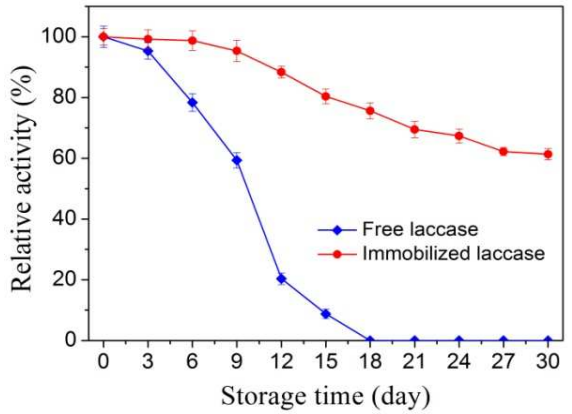

Fig. 8 The storage stability of free and immobilized laccase

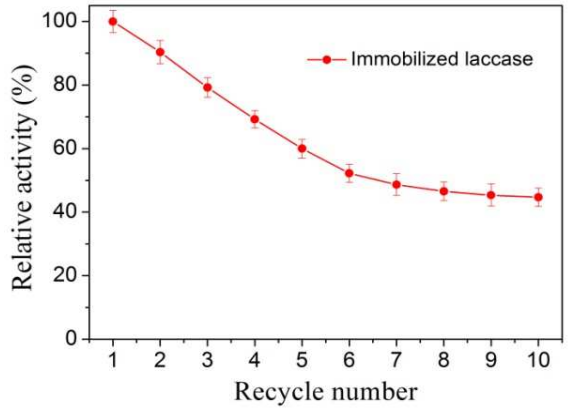

Fig. 9 The operational stability of immobilized laccase

The operational stability of the immobilized laccase was studied by cycles of ABTS oxidation because of its importance of application potential for reducing processing costs. The relative activity in each cycle of the immobilized laccase compared to the original activity on repeated use is shown in Fig. 9. The immobilized laccase could retain above 60% of its initial activity after 5 cycles of ABTS oxidation and separation using a magnet and over 40% after 10 cycles, which is in accordance with previous studies, where immobilized laccase on magnetic nanoparticles, magnetic nanoparticlesand magnetic mesoporous carbon were reported.[12,15,30] The results shown indicating a certain reusability of the laccase immobilized on AF-MSNPs. This reusability property of immobilized is essential for cost-effective use of the enzyme for biotechnological application.

3.4. Catalysing the oxidation of guaiacol by immobilized laccase

The immobilized laccase was used to calculate the catalytic efficiency of guaiacol, a typical phenolic lignin model compound. As shown in Fig. 10, the guaiacol was quickly oxidized by immobilized laccase and the maximal catalytic efficiency was obtained after 30 min (Fig. 10a) representing an excellent catalytic efficiency. The mechanism of catalytic the guaiacol by immobilized laccase was shown in Fig. 10b. The high catalytic efficiency of guaiacol indicating that utilizing the immobilized laccase to catalysis lignin is a very promising and novel technology for further application in the field of wood industry. By the radical polymerisation between the phenoxy radicals, the wood structure units such as wood fibers and particles can be bonded together under certain hot-pressing conditions and pressed into the eco-friendly wood-based composites without the emission of formaldehyde. The subsequent studies on manufacturing the eco-friendly wood-based composites using the immobilization laccase technology are being carried out.

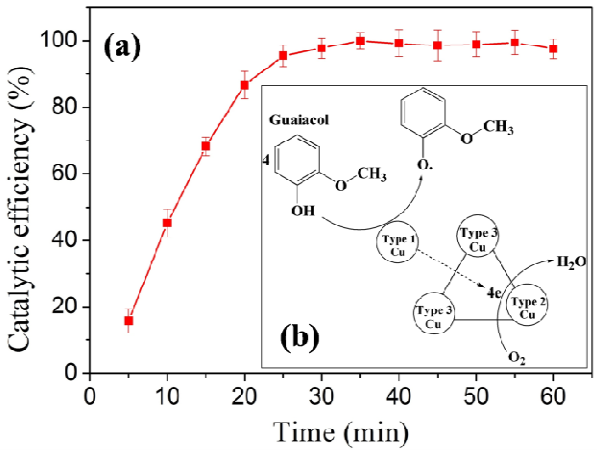

Fig. 10 Catalytic efficiency of guaiacol by immobilized laccase. (a) The curves of the catalytic efficiency as a function of time; (b) The mechanism of catalytic the guaiacol by immobilized laccase

Conclusions

In this work, we presented a facile and efficient method for *Aspergillus* laccase immobilization on magnetic silica nanoparticles by chemical crosslinking method. The results from FTIR, XRD, SEM and TEM characterizations indicated that the core-shell structure of the magnetic silica nanoparticles had been synthesized and successfully modified by APTES, which has laid a solid foundation for the laccase

immobilization. The average activity of the free and immobilized laccase was (1.465±0.025) × 10^{-3} U and (4.66±0.16) × 10^{-5} U/mg, respectively, and the immobilized exhibited 53.4±3.1 % of the total activity recovery. Compared to the free laccase, the lacase immobilized on AF-MSNPs not only exhibited better resistance to a broader pH and temperature value, but also exhibited significantly higher thermal stability, storage stability and operational stability of the biocatalysts. Furthermore, the immobilized laccase exhibited a high catalytic efficiency for oxidation of the guaiacol, a kind of lignin model compound, which indicated that utilizing the immobilized laccase to catalysis lignin, and through the radical polymerization to fabricate the wood-based composite materials, is a very promising and novel technology for further application in the field of wood industry.

Acknowledgements

This work was financially supported by the Special Fund for Forest Scientific Research in the Public Welfare (Grant No. 201404506), and the Fundamental Research Funds for the Central Universities (Grant No. 2572014AB13).

References

1 P. Li, H. L. Wang, G. S. Liu, X. Li and J. M. Yao, Enzyme Microb. Tech., 2011, **48**, 1-6.
2 J. Rotkova, R. Sulakova, L. Korecka, P. Zdrazilova, M. Jandova, J. Lenfeld, D. Horak and Z. Bilkova, J. Magn. Magn. Mater., 2009, **321**, 1335-1340.
3 P. Widsten and A. Kandelbauer, Enzyme Microb. Tech., 2008, **42**, 293-307.
4 P.Bajpai, Biotechnol. Progr., 1999, **15**, 147–57.
5 A.M.Mayer, R.C.Staples, Phytochemistry, 2002, **60**, 551–165.
6 A. Kharazipour, A. Huttermann, H. D. Ludemann, J. Adhes. Sci. Technol., 1997, **11**, 419–27.
7 M. Lund, M. Eriksson and C. Felby, Holzforschung, 2003, **57**, 21-26.
8 C. Felby, J. Hassingboe, M. Lund, Enzyme Microb. Tech., 2002, **31**, 736–741.
9 C. Felby, L. G. Thygesen, A. Sanadi and S. Barsberg, Ind. Crop. Prod., 2004, **20**, 181-189.
10 P. Widsten, J. E. Laine, S. Tuominen and P. Qvintus-Leino, J. Adhes. Sci. Technol., 2003, **17**, 67-78.
11 P. Widsten, S. Tuominen, P. Qvintus-Leino and J. E. Laine, Wood Sci. Technol., 2004, **38**, 521-528.
12 Y. Y. Liu, Z. T. Zeng, G. M. Zeng, L. Tang, Y. Pang, Z. Li, C. Liu, X. X. Lei, M. S. Wu, P. Y. Ren, Z. F. Liu, M. Chen and G. X. Xie, Bioresource Technol., 2012, **115**, 21-26.
13 A. P. M. Tavares, O. Rodriguez, M. Fernandez-Fernandez, A. Dominguez, D. Moldes, M. A. Sanroman and E. A. Macedo, Bioresource Technol., 2013, **131**, 405-412.
14 C. X. Ke, X. Li, S. S. Huang, L. Xu and Y. J. Yan, Rsc Adv., 2014, **4**, 57810-57818.
15 V. V. Kumar, S. Sivanesan and H. Cabana, Sci. Total Environ., 2014, **487**, 830-839.
16 Y. Zhang, G. M. Zeng, L. Tang, D. L. Huang, X.Y. Jiang and Y.N. Chen, Biosens. Bioelectron. 2007, **22**, 2121-2126.
17 S. Talekar, V. Ghodake, T. Ghotage, P. Rathod, P. Deshmukh, S. Nadar, M. Mulla and M. Ladole, Bioresource Technol., 2012, **123**, 542-547.
18 Z. Y. Lu, J. Dai, X. N. Song, G. Wang and W. S. Yang, Colloid. Surface. A, 2008, **317**, 450-456.
19 F. Wang, W. Huang, C. Guo and C. Z. Liu, Bioresource Technol., 2012, 126, 117-122.
20 W. Stober, A. Fink, E. Bohn, J. Colloid Interf. Sci., 1968, **26**, 62-69.
21 G. M. Ucoski, F. S. Nunes, G. DeFreitas-Silva, Y. M. Idemori and S. Nakagaki, Appl. Catal. A-Gen., 2013, **459**, 121-130.
22 P. A. Bazula, P. M. Arnal, C. Galeano, B. Zibrowius, W. Schmidt and F. Schuth, Micropor. Mesopor. Mat., 2014, **200**, 317-325.
23 R. Bourbonnais, M. G. Paice, Febs. Lett. 1990, **267**, 99-102.
24 H. Jung, F. Xu, K. C. Li, Enzyme Microb. Technol. 2002, **30**, 161-168.
25 S. X. Nie, X. L. Liu, Z. M. Wu, L. Zhan, G. D. Yin, S. Q. Yao, H. N. Song and S. F. Wang, Chem. Eng. J. 2014, **241**, 410-417.
26 D. R. Doerge, R. L. Divi and M. I. Churchwell, Anal. Biochem. 1997, **250**, 10-17.
27 Y. L. Lin, Y. Wei, Y. H. Sun and J. Wang, Mater. Res. Bull., 2012, **47**, 614-618.
28 T. Gholami, M. Salavati-Niasari, M. Bazarganipour and E. Noori, Superlattice. Microst., 2013, **6**1, 33-41.
29 X. D. Wang, Z. X. Shen, T. Sang, X. B. Cheng, M. F. Li, L. Y. Chen and Z. S. Wang, J. Colloid Interf. Sci., 2010, **341**, 23-29.
30 M. F. Deng, H. Zhao, S. P. Zhang, C. Y. Tian, D. Zhang, P. H. Du, C. M. Liu, H. B. Cao and H. P. Li, J Mol. Catal B-Enzym. 2015, **112**, 15-24.
31 M. Abdulla-Al-Mamun, Y. Kusumoto, T. Zannat, Y. Horie and H. Manaka, Rsc Adv., 2013, **3**, 7816-7827.
32 A. V. Blaaderen, J. V. Geest, A. Vrij, J. Colloid Interf. Sci., 1992, **154**, 481-501.
33 N. Plumere, A. Ruff, B. Speiser, V. Feldmann and H. A. Mayer, J. Colloid Interf. Sci., 2012, **368**, 208-219.
34 O. Barbosa, C. Ortiz, A. Berenguer-Murcia, R. Torres, R. C. Rodrigues and R. Fernandez-Lafuente, Rsc Adv. 2014, **4**, 1583-1600.
35 Y. Zhu, S. Kaskel, J. Shi, T. Wage and K. H. Van-Pee, Chem. Materi. 2007, **19**, 6408-6413.
36 H. Yavuz, G. Bayramoglu, Y. Kacar, A. Denizli and M. Y. Arica, Biochem. Eng. J. 2002, **10**, 1-8.
37 F. Wang, C. Guo, H. Z. Liu, C. Z. Liu, J Chem. Technol. Biot. 2008, **83**, 97-104.
38 M. Sari, S. Akgol, M. Karatas and A. Denizli, Ind. Eng. Chem. Res. 2006, **45**, 3036-3043.
39 F. Wang, C. Guo, L. Yang and C. Liu, Bioresource Technol. 2010, **101**, 8931-8935.
40 Y. Zhu, S. Kaskel, J. Shi, T. Wage and K. H. Van-Pee, Chem. Materi. 2007, **19**, 6408-6413.